



Contents lists available at SciVerse ScienceDirect

Physics Letters B

www.elsevier.com/locate/physletb

Temporal evolution of tubular initial conditions and their influence on two-particle correlations in relativistic nuclear collisions

R.P.G. Andrade^a, F. Grassi^{a,*}, Y. Hama^a, W.-L. Qian^b^a Instituto de Física, Universidade de São Paulo, Brazil^b Instituto de Ciências Exatas, Universidade Federal de Ouro Preto, Brazil

ARTICLE INFO

Article history:

Received 25 November 2011
Received in revised form 11 April 2012
Accepted 19 April 2012
Available online 23 April 2012
Editor: J.-P. Blaizot

Keywords:

Relativistic heavy-ion collisions
Particle correlations and fluctuations
Collective flow

ABSTRACT

Relativistic nuclear collisions data on two-particle correlations exhibit structures as function of relative azimuthal angle and rapidity. A unified description of these near-side and away-side structures is proposed for low to moderate transverse momentum. It is based on the combined effect of tubular initial conditions and hydrodynamical expansion. Contrary to expectations, the hydrodynamics solution shows that the high-energy density tubes (leftover from the initial particle interactions) give rise to particle emission in two directions and this is what leads to the various structures. This description is sensitive to some of the initial tube parameters and may provide a probe of the strong interaction. This explanation is compared with an alternative one where some triangularity in the initial conditions is assumed. A possible experimental test is suggested.

© 2012 Elsevier B.V. Open access under the [Elsevier OA license](#).

1. The need for a unified description

One of the most striking results in relativistic heavy-ion collisions at RHIC and the LHC, is the existence of structures in the two-particle correlations [1–8] plotted as function of the pseudo-rapidity difference $\Delta\eta$ and the angular spacing $\Delta\phi$. The so-called ridge has a narrow $\Delta\phi$ located around zero and a long $\Delta\eta$ extent. The other structure located opposite has a single or double hump in $\Delta\phi$. In order that two particles, emitted at some proper time $\tau_{f,out}$, appear as correlated over several rapidity units, the process that correlated them must have occurred [9,10] at a much smaller proper time due to causality. Therefore, the existence of long range pseudorapidity correlations must be related to early times in the nuclear collisions and thus has motivated many theoretical investigations.

Hydrodynamics has now been established as a good tool to describe many data from relativistic heavy-ion collisions so it should be able to provide a description for the above mentioned structures (for low to intermediate transverse momenta). In fact, as noted with RHIC data, a hydrodynamics based explanation is attractive because of the various similarities (see e.g. [11]) between bulk matter and ridge (transverse momentum spectra, baryon/meson ratio, etc.). In addition, it was shown (particularly at the LHC) that particle correlations can be understood in term of anisotropic flow Fourier coefficients [12–14]. This points towards

the necessity to have a *unified* hydrodynamic description of near- and away-side structures.

In early models, it was suggested that the combined effect of longitudinal high-energy density tubes (leftover from initial particle collisions) and transverse expansion was responsible for the ridge [15,16,9,10,17]. The particle emission associated to the tube was expected to occur in a single direction, so this would cause a ridge but no away-side structure. In addition, the effect of hydrodynamics was usually assumed to be of a certain type (e.g. a blast wave in [9,10,17]) and in fact when hydrodynamic expansion was actually computed, it seemed to lead to a disappearance of the initial high-energy density tubes [18] and therefore of their particle emission.

In a previous work [19], we presented evidence that hydrodynamics might in fact reproduce all structures using the NeXSPheRIO code. This code starts with initial conditions from the event generator NeXus [20] and solves the hydrodynamic equations on an event-by-event basis with the method of Smoothed Particle Hydrodynamics. In [19], the NeXSPheRIO events were analyzed in a similar way to the experimental ones, in particular the ZYAM method was used to remove effects of elliptic flow. We later developed a different method to remove elliptic flow from our data and checked that all structures were indeed exhibited and other features well reproduced (dependence on the trigger- or associated-particle transverse momentum, centrality, in-plane/out-of-plane trigger, appearance of a peak on the ridge). However, when using NeXSPheRIO, it is not clear how the various structures in the two-particle correlations are generated. The aim of this Letter is to investigate this, studying in detail what happens

* Corresponding author.

E-mail address: grassi@if.usp.br (F. Grassi).

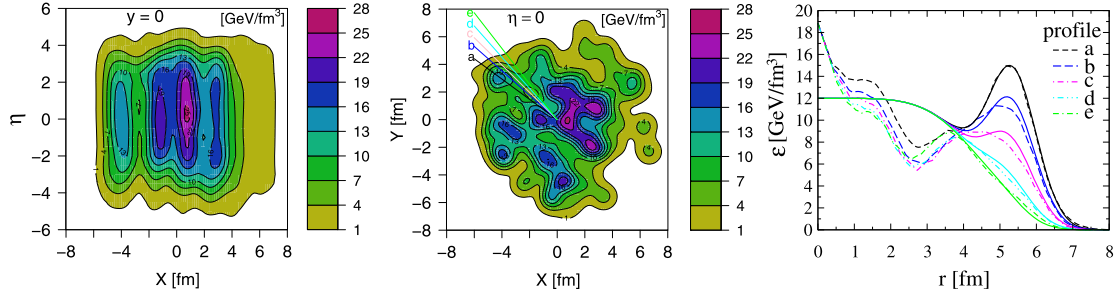


Fig. 1. Left and center: initial energy density for a NeXus central Au–Au collision at 200 GeV in the $y = 0$ and $\eta = 0$ plane respectively. Right: comparison of the parametrization given by Eq. (1) (solid lines) with the original NeXus energy density (dashed lines), along the lines a–e (in the $\eta = 0$ plane).

in the vicinity of an energetic tube (Section 2) and then extending the results to a more realistic complex case (Section 3). We will also compare our explanation with an alternative one that assumes some triangularity of the initial conditions (Section 4).

2. A simplified model

2.1. Origin of the near-side and away-side structures

We will consider central collisions only and use a simplified model. Fig. 1 (left and center) shows a typical example of initial conditions (initial energy density) obtained in NeXus with various tubular structures along the collision axis.

The origin of these structures is the following. To model soft physics in p–p collision, it is common to assume that strings (or color flux tubes) are formed, either via the excitation of the protons or due to color exchange between them. In A–A collisions, these strings may overlap leading to longitudinally extended regions of higher energy density such as those in Fig. 1. An alternative description of A–A collisions, based on gluon saturation, is that the two colliding nuclei can be viewed as Color Glass Condensates. Shortly after their collision, these produce strong color flux tubes called “Glasma”. Therefore the possibility that tubular structures exist in the initial conditions is general but their exact characteristics are not known.

In the simplified model, only one of the high-energy tubes from NeXus (chosen close to the border) is considered and the complex background is smoothed out. This leads to the following parametrization of the initial energy density

$$\epsilon = 12 \exp(-0.0004r^5) + \frac{34}{0.845\pi} \exp\left(\frac{-|\vec{r} - \vec{r}_0|^2}{0.845}\right), \quad (1)$$

where $r_0 = 5.4$ fm. A comparison of this parametrization with the original NeXus energy density is shown in Fig. 1 (right). Except for the inner region (which has little importance cf. Section 2.2), the agreement is reasonable. We use this parametrization in order to have a realistic tube description. However as already mentioned, the exact characteristics of the color tubes are not well known, therefore later we will consider various variations of the parameters.

In this simplified model or one-tube model, transverse expansion is computed numerically while longitudinal expansion is assumed boost-invariant, until freeze out at some constant temperature. The resulting single-particle angular distribution, shown in Fig. 2 (top), has two peaks located on both sides of the position of the tube (placed at $\phi = 0$) with separation ~ 2 (this is not a parameter), more or less independently of the value of the transverse momentum. Particle emission is computed assuming sudden freeze out. Since this is an approximation to real particle emission, we have checked that varying the freeze out temperature

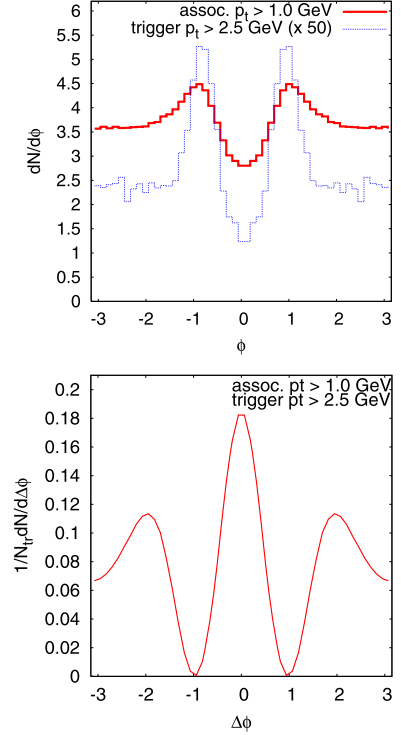


Fig. 2. Angular distributions of (direct) charged particles in some different p_T intervals (top) and resulting two-particle correlations (bottom) in the simplified model (for a freeze out temperature of 0.14 GeV).

(between 130 and 150 MeV) does not affect qualitatively our result.

This two-peak emission is in contrast with what happens when a blast wave is assumed, namely the fact that high-energy tubes emit in a single direction. However, its occurrence can be understood from Fig. 3. As time goes on, as a consequence of the tube expansion, a hole appears at the location of the high-energy tube (as in [18]). This hole is surrounded by matter that piles up in a roughly semi-circular cliff of high-energy density matter, guiding the flow of the background matter into two well-defined directions. The two extremities of the cliff emit more particles than the background, this gives rise to the two peaks in the single-particle angular distribution. The emission is not quite radial as shown by Fig. 3 (right), indicating that there was a deflection of the background flow due to the pressure exerted by the high-energy tube. As seen in Fig. 3, the fluid velocity is larger at the two extremities of the cliff and smaller nearby, this is why in Fig. 2 the angular distribution is narrower for larger p_T particles.

From Fig. 2 (top), we can guess how the two-particle angular correlation will be. The trigger particle is more likely to be in one

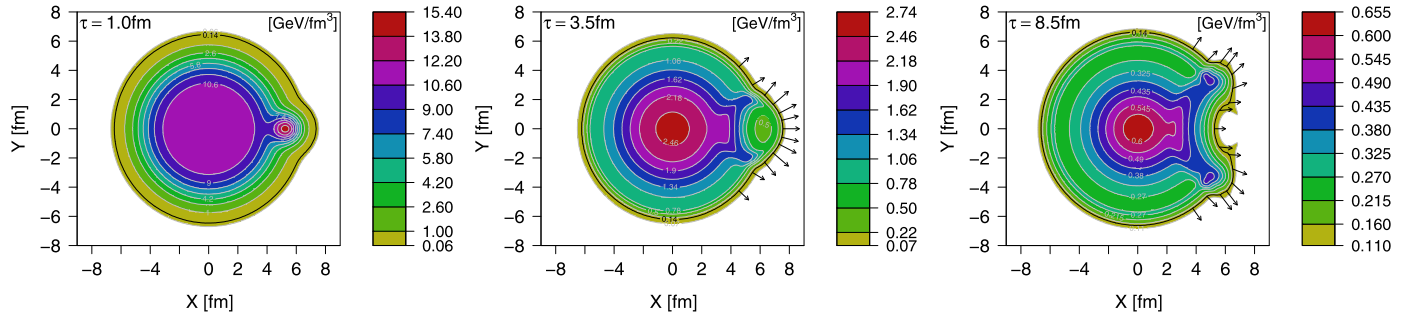


Fig. 3. Temporal evolution of energy density for the simplified model at times 1.0, 3.5 and 8.5 fm (thicker outer black curve corresponding to freeze out temperature of 0.14 GeV). Arrows indicate fluid velocity on the freeze out surface (vector length equivalent to 2 fm corresponds to light speed).

of the two peaks. We first choose the left-hand side peak. The associated particle is more likely to be also in this peak, i.e. with $\Delta\phi = 0$ or in the right-hand side peak with $\Delta\phi \sim +2$. If we choose the trigger particle in the right-hand side peak, the associated particle is more likely to be also in this peak, i.e. with $\Delta\phi = 0$ or in the left-hand side peak with $\Delta\phi \sim -2$. So the final two-particle angular correlation must have a large central peak at $\Delta\phi = 0$ and two smaller peaks respectively at $\Delta\phi \sim \pm 2$. Fig. 2 (bottom) shows that this is indeed the case. The peak at $\Delta\phi = 0$ corresponds to the near-side ridge and the peaks at $\Delta\phi \sim \pm 2$ form the double-hump ridge. We have checked [21] that this structure is robust by studying the effect of the height (12 ± 3 in the first term on the right-hand side of Eq. (1)) and shape of the background (r^5 to r^2 in the same term), overall initial transverse velocity (increasing radially up to 0.6), height, radius and location of the tube (some details are shown in the next section). The model was also generalized to non-central collisions and the in-plane/out-of-plane trigger dependence studied in [21].

2.2. Dependence on the tube parameters

In the above calculation, the tube extracted from NeXus initial conditions has a radius Δr of order 0.9 fm and (maximum) energy density ϵ_t of order 12 GeV fm^{-3} (at proper time 1 fm), as can be seen from the second term on the right-hand side of Eq. (1) or from Fig. 1. Changing Δr affects the height of the peaks and spacing in the two-particle correlation as shown in Fig. 4 (top). Changing ϵ_t has a similar strong effect. On the other side, if Δr and ϵ_t are changed maintaining constant the energy per unit length $E_t \propto \epsilon_t (\Delta r)^2$, as shown in Fig. 4 (bottom), the two-particle correlation maintains its overall shape, the angle between the peaks is almost unchanged and the peak heights change less. Therefore a good parameter to characterize the two-particle correlation is the tube total energy per unit length and tubes thinner than 0.9 fm are not excluded (see also [22]). For this comparison the background was kept unchanged, so the thinner tube energy density is really much higher than the background one, more realistic cases could be studied but this goes beyond the scope of this Letter.

The observation that the correlation is characterized by the energy per unit length E_t (not by Δr or ϵ_t separately) is consistent with the fact that what matters is the amount of energy available for the tube to push the surrounding matter. This also explains why the precise shape of the tube energy density (e.g. Gaussian as in Eq. (1)) is not crucial.

Finally, in Fig. 5, the tube is located (above the background) at various distances r_0 from the center, the height of the two-particle correlations at $\Delta\phi = 0$ saturates between 5.5 and 8 fm and decreases strongly for smaller distances to the center.

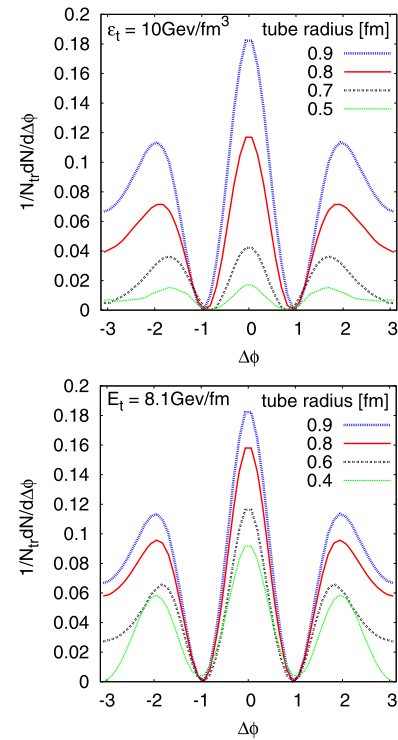


Fig. 4. Top: two-particle correlation for tubes with different radius but similar energy density. Bottom: two-particle correlation for tubes with different radius but similar energy content. (Tube position fixed at $r_0 = 5.4$ fm.)

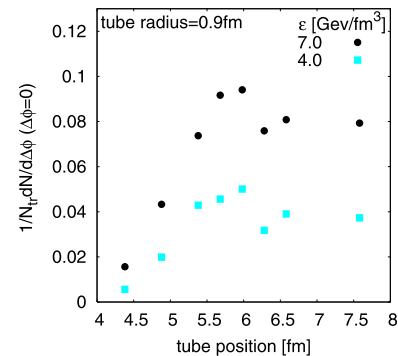


Fig. 5. Height of the two-particle correlation at $\Delta\phi = 0$ as function of the tube position with respect to the center.

The physical reason for the behavior of the maximum height of the two-particle correlation as function of the tube position can be understood by looking at the temporal evolution of the energy

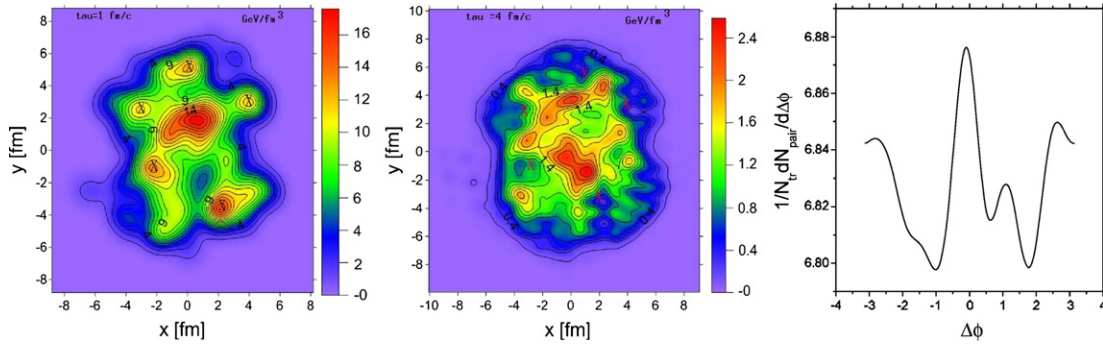


Fig. 6. Left: initial energy density for a NeXus central Au–Au collision at 200 GeV in the $\eta = 0$ plane with five outer tubes. Center: appearance of holes in the energy density during the temporal evolution (obtained assuming longitudinal boost invariance). Right: two-particle correlations.

density. When the tube is exactly at the center, there is no privileged direction of emission. When the tube is close to the outer border two privileged directions of emission appear (cf. Fig. 3). When the tube is at some small distance such as 2 fm, even though the strong expansion of the tube presses the surrounding matter creating a hole, this happens too much inside to cause the appearance of the two privileged directions of emission. We conclude, as mentioned earlier, that only peripheral tubes are important for the particle correlation.¹

3. More realistic case

With this information (and using the same two-dimensional hydrodynamic model as in previous section), we can discuss what happens in a more complex event such as a NeXus event. In such an event, only the outer tubes are expected to be relevant, for example in Fig. 6 (left), we can pinpoint five such tubes, indicated by crosses. When the time evolution of this matter slice is studied, holes appear in the vicinity of the former location of the tubes indicated by crosses in Fig. 6 (center). Due to expansion and the fact that one tube can interfere with another, we do not expect perfect one-to-one correspondence (though in this particular event, it is approximately the case).

The shape of the two-particle correlations for a single tube (in particular the peak spacing) is relatively independent of its features so the various tubes in the NeXus event under study will contribute with rather similar two-peak emission pattern at various angles in the single-particle angular distribution. As a consequence, the two-particle correlation of this NeXus event is expected to have a well-defined main structure similar to that of the one-tube model of the previous section (Fig. 2) surrounded by several other peaks and depressions due to trigger and associated particles coming from different tubes. This is indeed the case as shown in Fig. 6 (right). The additional peaks and depressions have positions depending on the angle of the tubes between them. When averaging over many events, these interference terms cancel out and only the main one-tube-like structure is left [19]. In other words: the picture derived in Section 2 also applies to more complex events such as NeXus ones.

4. Conclusion and perspectives

Usually, the initial conditions in the hydrodynamic description of relativistic nuclear collisions are assumed to be smooth.

It seems however that each time more, understanding data requires a knowledge of the fluctuating event-by-event initial conditions rather than an assessment of some adequate smooth initial conditions: fluctuations in elliptic flow [25] (perhaps the very behavior of elliptic flow as function of pseudorapidity [26]), Fourier coefficients of the azimuthal anisotropic flow (see below), two-particle correlations (see introduction).

In this Letter, a unified picture for the structures observed in two-particle correlations at low to moderate transverse momentum has been presented. It is based on the presence of longitudinal high-energy density tubes in the initial conditions. These tubes are leftover from the initial particle interactions. During the hydrodynamic evolution of the fluid, the strong expansion of the tubes located close to the border piles up matter in two symmetrical directions, leading to two-particle correlations with a near-side and a double hump away-side ridges (for central collisions).

An alternative unified picture has also been suggested, the idea is the following [27]. The ellipticity of the interaction region in a collision gives rise to elliptic flow because of the larger pressure gradients along the minor axis of the ellipse. Similarly, if the interaction region has some triangular shape, this causes triangular flow (due to existing larger pressure gradients in certain directions). Both near-side and double hump away-side ridges are a natural consequence of triangularity and triangular flow [27].

More generally, it has been suggested that the initial transverse density in the overlap region can be decomposed using an infinite set of moments and any observable (in particular anisotropic flow Fourier coefficients v_n) can be written as a function of these moments [28]. Conventional eccentricities such as ellipticity and triangularity, are basically a subset of these moments, which may or not be sufficient to characterize the v_n 's (see e.g. [29]).

Both tube configuration such as in this Letter and triangularity [27] (or more general geometrical shape of the interaction region) lead to non-zero eccentricities. In the case of NeXus, these eccentricities reflect the initial conditions where a lot of peaks or “hot spots” and valleys are present as can be seen in Figs. 1 and 6 (similar features can be seen in EPOS initial conditions [22]). On the other side, depending on the sampling process for the nucleon–nucleon collisions and sources of fluctuations included, the interaction region may present a geometrical shape without dominance of a few tubes and might be described by conventional eccentricities such as suggested in [27].

The hydrodynamical response to the anisotropies differs in the two cases. In our description, the structures in the two-particle correlations and the various v_n 's are a response to individual *outer* tubes: this is a local effect. In the case of triangularity (or more general geometrical shape) of the interaction region, the structures in the two-particle correlations and v_n 's correspond to the various geometrical deformations: this is a global effect. In our approach,

¹ An opposite conclusion was reached in Fig. 10 of [23]. A possible explanation for this discrepancy, is that they use the Gubser solution which has some unphysical features at large radii as discussed in [24] (in particular see Fig. 3 there).

the angular size of the near-side ridge, ~ 2 , is of local hydrodynamic origin and can be roughly understood as the diameter of the hole divided by the radius of the nucleus, i.e. $2c_s\tau_{f.out}/R$ (ignoring the non-radial flow of particle emission cf. Section 2.1). In the triangularity case, this angular size is fixed by global geometry (for example $2\pi/3$ in the simple case of an equilateral triangular shape). Similarly, in our approach, the relative height of the peaks in the two-particle correlation is of local hydrodynamical origin: for example, for a single tube (in a central collision), the highest peak is approximately twice higher than the two smaller peaks (cf. Fig. 2). In the triangularity case, the relative height of the peaks in the two-particle correlation is related to global geometry: for example, in the simple case of an equilateral triangular shape, there should be three equal height peaks in the two-particle correlation. However, to turn the connection between initial (local or global) geometry and flow more precise, pre-equilibrium evolution [30] and viscosity [31] should be included since both, though they are small effects, can smear out the initial anisotropies.

Finally, to further test the presence of tubular structures in the initial conditions, we suggest to build 2+1 correlations, fixing both a trigger particle and a first associated particle, this last one with $\Delta\phi_1 \sim 2$. This choice ensures that both particles come from different emission peaks in the single-particle angular distribution. Then, in our approach, the second associated particle will be more likely to come from the same emission peak as the trigger, i.e. with $\Delta\phi_2 = 0$ or the same emission peak as the first associated particle, i.e. with $\Delta\phi_2 \sim 2$. Naively, the plot of the 2+1 correlation as function of $\Delta\phi_2$ vs. $\Delta\eta_2$ should present two stripes located at $\Delta\phi_2 = 0$ and $\Delta\phi_2 \sim 2$. However, in practice, there appears a third weaker stripe, due to the background. In the eccentricity case, the plot is expected to be more complicated (in the simple case of only equilateral triangular shapes – with longitudinal extension, there should be three equally bright stripes). Additional work with realistic initial conditions is needed to check whether 2+1 correlations may indeed permit to distinguish between both scenarios.

Since the two scenarios, isolated tube configuration such as in this Letter and triangularity (or more general geometrical shape of the interaction region) correspond to different schemes of initial

state energy deposition, distinguishing between them may allow to learn about how the strong interaction proceeds during high-energy nuclear collisions.

Acknowledgements

We acknowledge funding from CNPq and FAPESP.

References

- [1] A. Adare, et al., PHENIX Collaboration, Phys. Rev. C 78 (2008) 014901.
- [2] B.I. Abelev, et al., STAR Collaboration, Phys. Rev. Lett. 102 (2009) 052302.
- [3] B.I. Abelev, et al., STAR Collaboration, Phys. Rev. C 80 (2009) 064912.
- [4] B. Alver, et al., PHOBOS Collaboration, Phys. Rev. C 81 (2010) 024904.
- [5] B. Alver, et al., PHOBOS Collaboration, Phys. Rev. Lett. 104 (2010) 062301.
- [6] K. Aamodt, et al., ALICE Collaboration, Phys. Rev. Lett. 107 (2011) 032301.
- [7] B. Wyslouch, for the CMS Collaboration, J. Phys. C 38 (2011) 124005.
- [8] P. Steinberg, for the ATLAS Collaboration, J. Phys. C 38 (2011) 124004.
- [9] A. Dumitru, et al., Nucl. Phys. A 810 (2008) 91.
- [10] S. Gavin, et al., Phys. Rev. C 79 (2009) 051902.
- [11] B. Mohanty, for the STAR Collaboration, J. Phys. G 35 (2008) 104006.
- [12] ALICE Collaboration, arXiv:1109.2501, 2011.
- [13] ATLAS Collaboration, arXiv:1109.6721, 2011.
- [14] CMS Collaboration, arXiv:1201.3158, 2012.
- [15] S. Voloshin, Phys. Lett. B 632 (2006) 490.
- [16] E. Shuryak, Phys. Rev. C 76 (2007) 047901.
- [17] G. Moschelli, S. Gavin, arXiv:0910.3590v2, 2009.
- [18] E. Shuryak, Phys. Rev. C 80 (2009) 054908.
- [19] J. Takahashi, B.M. Tavares, W.-L. Qian, R. Andrade, F. Grassi, Y. Hama, T. Kodama, N. Xu, Phys. Rev. Lett. 103 (2009) 242301.
- [20] H.J. Drescher, F.M. Liu, S. Ostapchenko, T. Pierog, K. Werner, Phys. Rev. C 65 (2002) 054902.
- [21] R.P.G. Andrade, PhD thesis, 2011.
- [22] K. Werner, Iu. Karpenko, T. Pierog, M. Bleicher, K. Mikhailov, Phys. Rev. C 82 (2010) 044904.
- [23] P. Staig, E. Shuryak, arXiv:1105.0676v2, 2011.
- [24] S.S. Gubser, Phys. Rev. D 82 (2010) 085027.
- [25] Y. Hama, R.P.G. Andrade, F. Grassi, W.-L. Qian, T. Osada, C.E. Aguiar, T. Kodama, Phys. Atom. Nucl. 71 (2008) 1558.
- [26] R.P.G. Andrade, F. Grassi, Y. Hama, T. Kodama, W.-L. Qian, Phys. Rev. Lett. 101 (2008) 112301.
- [27] B. Alver, G. Roland, Phys. Rev. C 81 (2010) 054905.
- [28] D. Teaney, L. Yan, Phys. Rev. C 83 (2011) 064904.
- [29] F.G. Gardim, F. Grassi, M. Luzum, J.-Y. Ollitrault, Phys. Rev. C 85 (2012) 024908.
- [30] G.-Y. Qin, H. Petersen, S.A. Bass, B. Müller, Phys. Rev. C 82 (2010) 064903.
- [31] B. Schenke, S. Jeon, C. Gale, Phys. Rev. Lett. 106 (2011) 042301.